




Physical modelling of energy losses at surcharged three-way junction manholes in drainage system

Q. Li ^a, J. Xia ^{a,*}, M. Zhou^a, S. Deng^a, H. Zhang ^b and Z. Xie^c

^a State Key Laboratory of Water Resources and Hydropower Engineering Science, Wuhan University, Wuhan 430072, China

^b Faculty of Advanced Science and Technology, Kumamoto University, Kumamoto 860-8555, Japan

^c School of Engineering, Cardiff University, Cardiff CF24 3AA, United Kingdom

*Corresponding author. E-mail: xiajq@whu.edu.cn

 QL, 0000-0001-7840-1750; JX, 0000-0001-7613-3457; HZ, 0000-0003-0335-7999

ABSTRACT

Motivated by the observation that vortex flow structure was evident in the energy loss at the surcharged junction manhole due to changes of hydraulic and geometrical parameters, a physical model was used to calculate energy loss coefficients and investigate the relationship between flow structure and energy loss at the surcharged three-way junction manhole. The effects of the flow discharge ratio, the connected angle between two inflow pipes, the manhole geometry, and the downstream water depth on the energy loss were analyzed based on the quantified energy loss coefficients and the identified flow structure. Moreover, two empirical formulae for head loss coefficients were validated by the experimental data. Results indicate that the effect of flow discharge ratio and connected angle are significant, while the effect of downstream water depth is not obvious. With the increase of the lateral inflow discharge, the flow velocity distribution and vortex structure are both enhanced. It is also found that a circular manhole can reduce local energy loss when compared to a square manhole. In addition, the tested empirical formulae can reproduce the trend of total head loss coefficient.

Key words: energy loss, hydrodynamics, sewer pipe, surcharged manhole, three-way junction, urban drainage

HIGHLIGHTS

- Experimental study on energy losses at surcharged three-way junction manholes.
- Effects of the flow discharge ratio, the connected angle between two inflow pipes, and the manhole geometry were analyzed based on the quantified energy loss coefficients and the identified flow structure.
- Empirical head loss coefficient formulae were validated by experimental data.

1. INTRODUCTION

With global warming and the acceleration of urbanization, existing storm sewer systems in urban areas are frequently overloaded due to insufficient drainage capacity (Chang *et al.* 2013). This may cause serious problems such as sewer pipe rupture, blown-off manhole covers, soil erosion, and urban flooding (Jo *et al.* 2018; Crispino *et al.* 2019b; Crispino *et al.* 2021). For instance, the cover of a three-way junction manhole was blown off during the storm 2016 in the city of Wuhan, China. The precise indication of the places where water spills over through manholes of the storm sewer networks is necessary to reduce urban flood risk. Therefore, it is crucial to study drainage capacity for preventing urban flooding (Ruggaber *et al.* 2007; Borsányi *et al.* 2008; Granata *et al.* 2014).

In urban areas, manholes connecting sewer pipes at pipes joints are essential parts in the drainage system especially during urban flooding due to their importance in sewer maintenance, sewer connection, and diversion function (Crispino *et al.* 2015; Zhang *et al.* 2018, 2020). It has been found that manhole energy loss plays a significant role in drainage capacity (Stovin *et al.* 2013). The increased energy loss at a surcharged junction manhole reduces the capacity of the drainage system (Wang *et al.* 1998; Tavakol *et al.* 2016). Over the past few decades, many efforts have been made to study energy loss at the surcharged junction manholes based on physical models (Del Giudice *et al.* 2000; Pfister & Gisonni 2014; Zhu *et al.* 2016; Rubinato *et al.* 2017, 2018a, 2018b; Jo *et al.* 2018; Crispino *et al.* 2019a, 2019b, 2021; Lin *et al.* 2020). Study on head loss coefficient

This is an Open Access article distributed under the terms of the Creative Commons Attribution Licence (CC BY-NC-ND 4.0), which permits copying and redistribution for non-commercial purposes with no derivatives, provided the original work is properly cited (<http://creativecommons.org/licenses/by-nc-nd/4.0/>).

calculation and head loss reduction in surcharged manholes with different manhole shapes and benching floor configurations was conducted by (Marsalek 1984). Energy losses at a surcharged two-way junction manhole with a main inflow pipe and a 90° lateral inflow pipe were measured by Lindvall (1984). A comprehensive experiment was conducted to investigate the local head losses of combining flows at junction manholes for free surface flows in circular conduits, with various diameters and in the presence of sub- and super-critical approaching flows (Pfister & Gisonni 2014). Wave configurations of supercritical junction manholes were investigated by Del Giudice *et al.* (2000) and Gisonni & Hager (2002). A series of laboratory experiments were conducted by (Zhang *et al.* 2020) to study the hydraulic properties of three-way manhole junctions. Study of energy dissipation in a circular drop manhole with different flow patterns and drop heights was conducted by Granata *et al.* (2014) and Zheng *et al.* (2017). Results show that various parameters affect the hydraulic performance of the drop manhole. Kim *et al.* (2018) used a physical model to derive efficient benching designs that can reduce head loss. Results indicate that the installation of full rectangular benching reduced the head loss coefficients and can be installed to improve the drainage capacity of urban stormwater conduit facilities. Based on the experimental datasets, several types of theoretical formulae for energy loss coefficients have been proposed. One representative head loss coefficient formula guideline was proposed in the urban drainage design manual (UDDM) by the federal highway administration (FHWA 2009). Following this guideline, an alternative formula was proposed for three-way manholes under surcharged conditions by considering more variables of structural elements for the pipes and the manholes (Arao *et al.* 2016). In the proposed formula, the effect of diameter ratios between inflow and outflow pipes, flow rate ratios between inflow pipes, connected angle between inflow pipes, and drop gaps between inflow pipes and outflow pipe were included.

Currently, there is limited existing work investigating the flow structure and the influence of hydrodynamic force on energy loss in the surcharged three-way manhole system. Moreover, it is also observed that the head loss coefficient at manholes is usually neglected in floods analysis model due to the lack of validated theoretical formulae. To improve the reliability of the flood modelling, it is necessary to evaluate the risk of manhole failure quantitatively with efficient and accurate theoretical formulae of energy loss coefficients in the manhole. Therefore, more validations are needed to examine the existing empirical formulae.

The objective of this study is to use a physical model to investigate the influencing factors of local energy loss at the surcharged three-way junction manhole not only by calculating the energy loss coefficients, but also by calculating hydrodynamics and identifying flow structures in the manhole. In addition, two representative empirical formulae for energy loss coefficients were examined based on the experimental datasets. The paper is organized as follows: In section 2, an introduction of the physical model is given. In section 3, theoretical background of energy loss coefficients and hydrodynamic force are presented. Results and discussion are demonstrated in section 4. Finally, conclusions and future works are summarized in section 5.

2. EXPERIMENTS

2.1. Physical model

The physical model (Figure 1(a)) was operated at the Ujigawa Open Laboratory, Disaster Prevention Research Institute of Kyoto University. The three-way junction manhole is sketched in Figure 1(b). It consists of two upstream pipes including a straight inflow pipe and a lateral inflow pipe, all having circular cross-section of diameters $D_1 = D_2 = 0.05$ m. The connected angle θ between two inflow pipes can be adjusted. There is a downstream outflow pipe with a circular cross-section of diameter $D_3 = 0.05$ m. The manhole diameter B is 0.15 m. Discharge of the straight inlet flow Q_1 , lateral inlet flow Q_2 , and outlet flow pipes Q_3 are recorded by three electro-magnetic flow meters (Yokogawa Electric ADMAG AXF) located in the upstream of the inlet pipes and the downstream of the outlet pipe, respectively. h_m is the water depth in the manhole and h_d is the water depth in the downstream tank. The piezometric heads at representative locations in the pipes are measured with a sequence of customized piezometers as shown in Figure 1(b). In the upstream of the pipeline system, there are two tanks which supply water to the straight and lateral inlet pipes, respectively. At the downstream of the outlet pipe, there is a tank and a reservoir. Water is pumped from the downstream reservoir to the upstream tanks. The flow discharge is adjustable through a pump-valve system. The pipe flow is pressurized flow and the flow in the manhole is free surface flow. The manhole, the sewer pipes, the tanks, and the reservoir are made from transparent acrylic materials. The sewer pipes are arranged horizontally in the experiments.

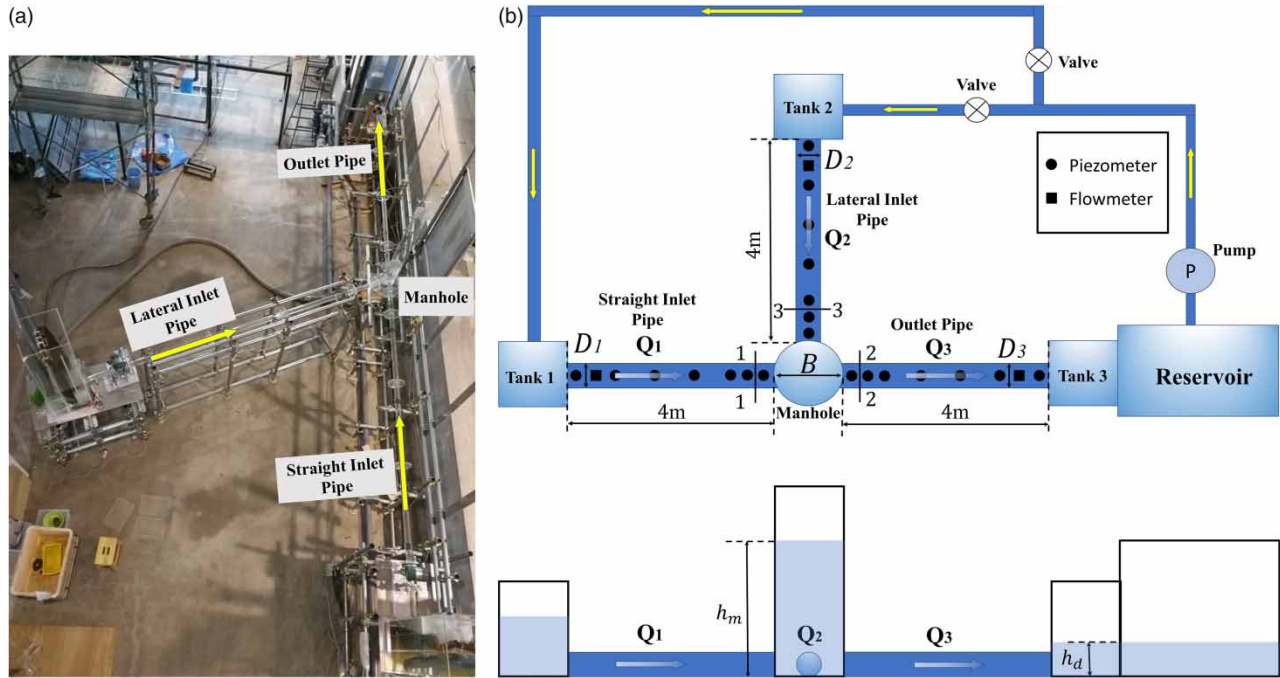


Figure 1 | Schematic and configurations of the physical model: (a) physical model of three-way junction manhole; (b) plan and side views of the experiment setup.

Flow features in the manhole were investigated by a Particle Image Velocimetry (PIV) system as shown in Figure 2. A laser (DPGL-2 W, Japan Laser, Co., Ltd) and a high-speed camera (FASTCAM Mini UX50, Photron Limited) were used to record the flow motion in horizontal and vertical cross-sections of the manhole as shown in Figure 2(a) and 2(b), respectively. The position of the high-speed camera and the laser are perpendicular to each other. When measuring the horizontal cross-section, the high-speed camera is placed at the vertical position of the section, that is, directly under the manhole model as shown in Figure 2(a). For vertical cross-section measurement, the PIV laser is located directly below the manhole model as shown in Figure 2(b). When using PIV technology to measure flow velocity, it is necessary to evenly put tracer particles with good flowability and astigmatism into the two-dimensional flow field. The specific gravity of the tracer particles is

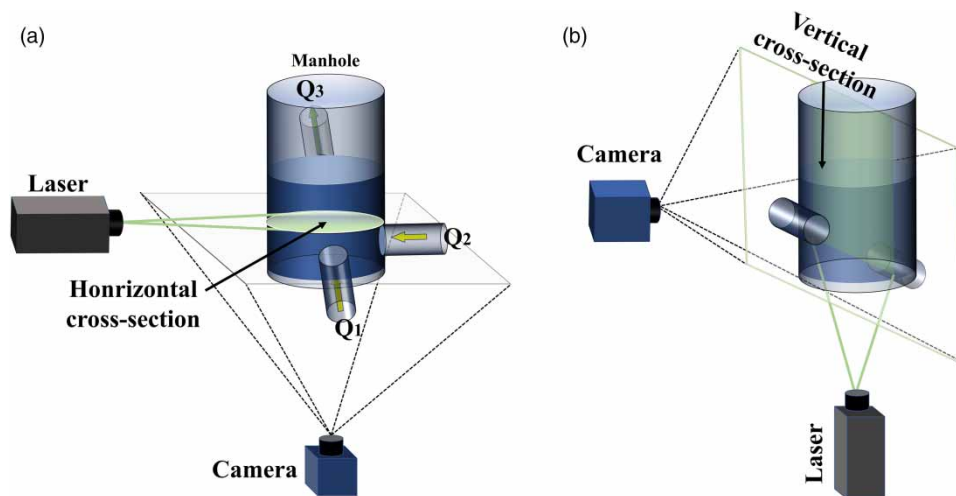


Figure 2 | The schematic of the PIV system for the cross-sections of the manhole: (a) horizontal cross-section; (b) vertical cross-section.

equivalent to that of the fluid, so it will not interfere with the water flow field. A piece of light source with a thickness of about 1 mm is injected into the area to be measured in the flow field. The piece of the light source is formed by the light beam generated by the laser after being scattered by the lens. The lens distortion effect was removed from the images by warping the frames based on the use of a calibration chequerboard image. Pixels outside the measurement area were cropped for each image. Before each test, the mean 'background' (i.e., with no seeding particles) image was recorded over 3 minutes. The subsequent PIV instantaneous images were then subtracted from this background, such that the background would turn black while the particles would remain white. Seeding particles were applied to the flow via an upstream roller brush attached to a vibrating particle hopper. Measurements were recorded for a period of 3 minutes for each test. The obtained images were analyzed using the commercial PIV software (Flow Expert 2D2C, Katokoken Co., Ltd) and an adaptive correlation was performed to determine the velocity field for each time adjacent image pair.

2.2. Experimental conditions

For this physical model, the flow discharge in the inlet pipes varied from 0 L/s to 3 L/s, while the flow discharge in the outlet pipe was kept as a constant of 3 L/s. The ratio of flow discharge Q_2/Q_3 was set from 0 to 1.0. Downstream flow height varies from 0.025 m to 0.1 m. The connected angle θ between two inflow pipes can be adjusted. Square and circular cross-section manholes were compared. Detailed experimental conditions of the model are outlined in Table 1.

3. THEORETICAL BACKGROUND

3.1. Head loss coefficients

The flow in the surcharged three-way manhole system follows the conservation laws of mass, momentum, and energy. The continuity equation is:

$$Q_3 = Q_1 + Q_2 \quad (1)$$

where Q_1 and Q_2 are flow discharge of the straight inflow pipe and lateral inflow pipe, respectively. Q_3 is the outflow discharge. To describe the local energy losses induced by the junction manhole with two inlet sections and one outlet section, the energy balance equation (Wang *et al.* 1998) can be defined as follows:

$$\rho g(H_1 Q_1 + H_2 Q_2) - \rho g(H_3 Q_3) = \rho g(\Delta H Q_3) \quad (2)$$

where H_1 and H_2 refer to the total head corresponding to the main inflow pipe and lateral inflow pipe, respectively. H_3 is the total head of the outflow pipe and ΔH is the local head loss in the manhole. ρ is the density of water and g is the acceleration of gravity. Local heads H_i ($i = 1, 2, 3$) at each pipe is calculated by

$$H_i = \frac{V_i^2}{2g} + h_i \quad (3)$$

where V_i is the mean flow velocity over the cross-section flow at the reference point i (m/s), h_i is the pressure head at the

Table 1 | Manhole shapes and physical model study conditions

Manhole Type	θ (degree)	h_d (m)	Q_1 (L/s)	Q_2 (L/s)	Q_3 (L/s)	Inlet pipe 1 Re	Inlet pipe 2 Re	Inlet pipe 3 Re
Square	45	0.050	3.0	0.0	3.0	7.60×10^4	0	7.60×10^4
	60	0.075	2.0	1.0	3.0	5.07×10^4	3.80×10^4	7.60×10^4
Circular	90	0.100	1.0	2.0	3.0	2.53×10^4	5.07×10^4	7.60×10^4
			0.0	3.0	3.0	0	7.60×10^4	7.60×10^4

reference point i (m). Substituting Equation (3) into Equation (2), we can obtain:

$$Q_3 \Delta H = Q_1 \left(\frac{V_1^2}{2g} + h_1 \right) + Q_2 \left(\frac{V_2^2}{2g} + h_2 \right) - Q_3 \left(\frac{V_3^2}{2g} + h_3 \right) \quad (4)$$

Given the continuity Equation (1), the local energy loss at the manhole described in Equation (4) essentially consists of local energy loss from the straight inflow pipe and the lateral inflow pipe, which yields:

$$Q_3 \Delta H = Q_1 \Delta H_1 + Q_2 \Delta H_2 \quad (5)$$

ΔH_1 and ΔH_2 refer to the local head loss corresponding to the straight inflow pipe and lateral inflow pipe, respectively. The head loss term ΔH_i ($i = 1, 2$) can be expressed as the product of a dimensionless head loss coefficient K_i ($i = 1, 2$) and the velocity head of outlet flow as follows:

$$\Delta H_i = K_i \cdot H_0, \quad (i = 1, 2) \quad (6)$$

where $H_0 = \frac{V_3^2}{2g}$ is the head corresponding to the outlet pipe. The head loss coefficient between the straight inlet pipe and the outlet pipe K_1 can be written as:

$$K_1 = \Delta H_1 / H_0 = (H_1 - H_3) / H_0 \quad (7)$$

Analogously, the head loss coefficient between the lateral inlet pipe and the outlet pipe K_2 can be written as:

$$K_2 = \Delta H_2 / H_0 = (H_2 - H_3) / H_0 \quad (8)$$

The total head loss coefficient K in the manhole can be written as:

$$K = \Delta H / H_0 = \frac{Q_1}{Q_3} K_1 + \frac{Q_2}{Q_3} K_2 \quad (9)$$

In previous works, several types of empirical formulae of head loss coefficients have been proposed to reproduce energy loss at junction manholes (Lindvall 1984; Marsalek 1984; FHWA 2009; Arao *et al.* 2016). In this work, two empirical formulae were examined for the three-way junction manhole. The first empirical formula was proposed in the urban drainage design manual (UDDM) (FHWA 2009), which can be described as:

$$K_i = K_0 C_D C_d C_Q, \quad (i = 1, 2) \quad (10)$$

where

$$K_0 = 0.1 \left(\frac{B}{D_3} \right) (1 - \sin \theta_i) + 1.4 \left(\frac{B}{D_3} \right)^{0.15} \sin \theta_i \quad (11)$$

$$C_D = \left(\frac{D_3}{D_i} \right)^3 \quad (12)$$

$$C_d = 0.5 \left(\frac{h_m}{D_3} \right)^{0.6}, \quad \left(\frac{h_m}{D_3} > 3.2, C_d = 1 \right) \quad (13)$$

$$C_Q = (1 - 2 \sin \theta_i) \left(1 - \frac{Q_i}{Q_3} \right)^{0.75} + 1 \quad (14)$$

The second empirical formula was designed by *Arao et al. (2016)*, which can be described as:

$$K_i = K_0 C_{Q_i} \quad (15)$$

where

$$K_0 = 0.702 \left(\frac{B}{D_3} \right)^{0.63} \quad (16)$$

$$C_{Q_1} = \begin{cases} [1.1032 - 1.494(1 - \sin\theta_1)] \left(\frac{Q_1}{Q_3} - 0.5 \right) + 0.4, & 0.5 \leq \frac{Q_1}{Q_3} \leq 1 \\ [-0.2232 - 1.6(1 - \sin\theta_2)] \left(0.5 - \frac{Q_1}{Q_3} \right) + 0.4, & 0 \leq \frac{Q_1}{Q_3} \leq 0.5 \end{cases} \quad (17)$$

$$C_{Q_2} = \begin{cases} [1.1032 - 1.494(1 - \sin\theta_2)] \left(\frac{Q_2}{Q_3} - 0.5 \right) + 0.4, & 0.5 \leq \frac{Q_2}{Q_3} \leq 1 \\ [-0.2232 - 1.6(1 - \sin\theta_1)] \left(0.5 - \frac{Q_2}{Q_3} \right) + 0.4, & 0 \leq \frac{Q_2}{Q_3} \leq 0.5 \end{cases} \quad (18)$$

3.2. Hydrodynamic force in junction manhole

The momentum conservation equation in the outflow direction is:

$$\rho Q_1 V_1 + \rho Q_2 V_2 - \rho Q_3 V_3 = P_3 A_3 - P_1 A_1 - P_2 A_2 \cdot \cos\theta + F \quad (19)$$

where A_1 , A_2 , and A_3 are the cross-sectional area of the straight inflow pipe, the lateral inflow pipe, and the outflow pipe, respectively. In this study, $A_1 = A_2 = A_3 = 0.002 \text{ m}^2$. P_1 , P_2 , and P_3 are the pressure head in the straight inflow pipe, the lateral inflow pipe, and the outflow pipe, respectively.

$$V_1 = \frac{Q_1}{A_1}, \quad V_2 = \frac{Q_2}{A_2}, \quad V_3 = \frac{Q_3}{A_3} \quad (20)$$

$$P_1 = \rho g h_1, \quad P_2 = \rho g h_2, \quad P_3 = \rho g h_3 \quad (21)$$

Substituting Equations (20) and (21) into Equation (19), and separating the hydrodynamic force term F from Equation (19), the hydrodynamic force F is obtained:

$$F = \frac{\rho}{A^2} (Q_1^2 + Q_2^2 - Q_3^2) - \rho g A (h_3 - h_1 - h_2 \cdot \cos\theta) \quad (22)$$

4. RESULTS AND DISCUSSION

4.1. Effect of downstream water depth on manhole energy loss

The relationships between head loss coefficients (K , K_1 , and K_2) and the downstream water depth (h_d) in different flow discharge ratio (Q_2/Q_3) conditions are shown in [Figure 3](#). Results show that there is a slight variance of the total energy loss coefficients at the junction manhole with the change of downstream water depth, especially for K and K_2 . Overall, the effect of downstream water depth on manhole local energy loss is not obvious.

4.2. Effect of flow discharge ratio on manhole energy loss

[Figure 4](#) shows the manhole head loss coefficients K , K_1 , and K_2 with flow discharge ratio Q_2/Q_3 for $\theta = 45^\circ$, $\theta = 60^\circ$, and $\theta = 90^\circ$, respectively. It is found that K and K_2 are consistently increased with the increase of Q_2/Q_3 . When $Q_2/Q_3 > 2:3$, the inlet flow rate ratio was dominated by the lateral inlet pipe, and the total head loss coefficient K increases significantly. However, it is observed that the trend of K_1 is different compared to that of K and K_2 . When $\theta = 60^\circ$ and $\theta = 90^\circ$, K_1 increases continuously with the increase of Q_2/Q_3 . However, when $\theta = 45^\circ$, K_1 varies between peak and valley values.

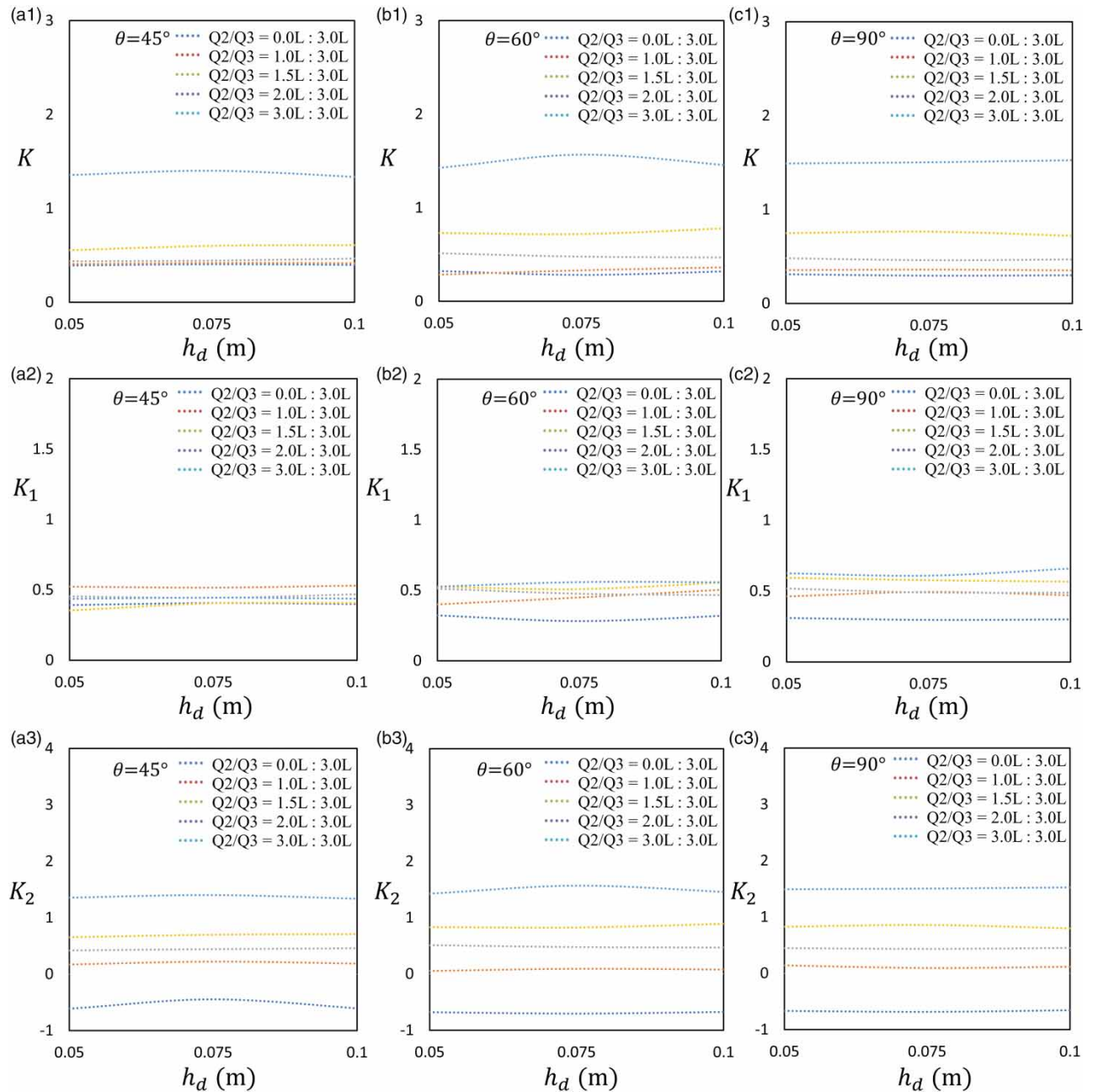


Figure 3 | The head loss coefficients K , K_1 , and K_2 with downstream water depth h_d in different flow discharge ratios Q_2/Q_3 . (a1), (a2), and (a3) represent the head loss coefficient K , K_1 , and K_2 according to $\theta = 45^\circ$. (b1), (b2), and (b3) represent the head loss coefficient K , K_1 , and K_2 according to $\theta = 60^\circ$. (c1), (c2), and (c3) represent the head loss coefficients K , K_1 , and K_2 according to $\theta = 90^\circ$.

Figure 5 shows the dynamic force F and manhole water depth h_m with a flow discharge ratio Q_2/Q_3 for $\theta = 45^\circ$, $\theta = 60^\circ$, and $\theta = 90^\circ$, respectively. It is found that both of F and h_m are consistently increased with the increase of the flow discharge ratio. This trend is consistent with the total head loss coefficients K . With the increase of the velocity in the lateral pipe, the water depth in the junction manhole was increased due to the increased velocity head transfers to the pressure head.

To further investigate the flow details in the junction manhole, Figures 6 and 7 present the velocity distribution and flow streamline in horizontal and vertical cross-sections at the junction manhole. It is observed that when the flow discharge ratio Q_2/Q_3 is increased from 1/3 to 1/2, the velocity distribution in horizontal and vertical cross-sections expanded with increased values and the vortex structure (streamline in ellipse dotted line) is also enhanced. Therefore, the total energy loss at the

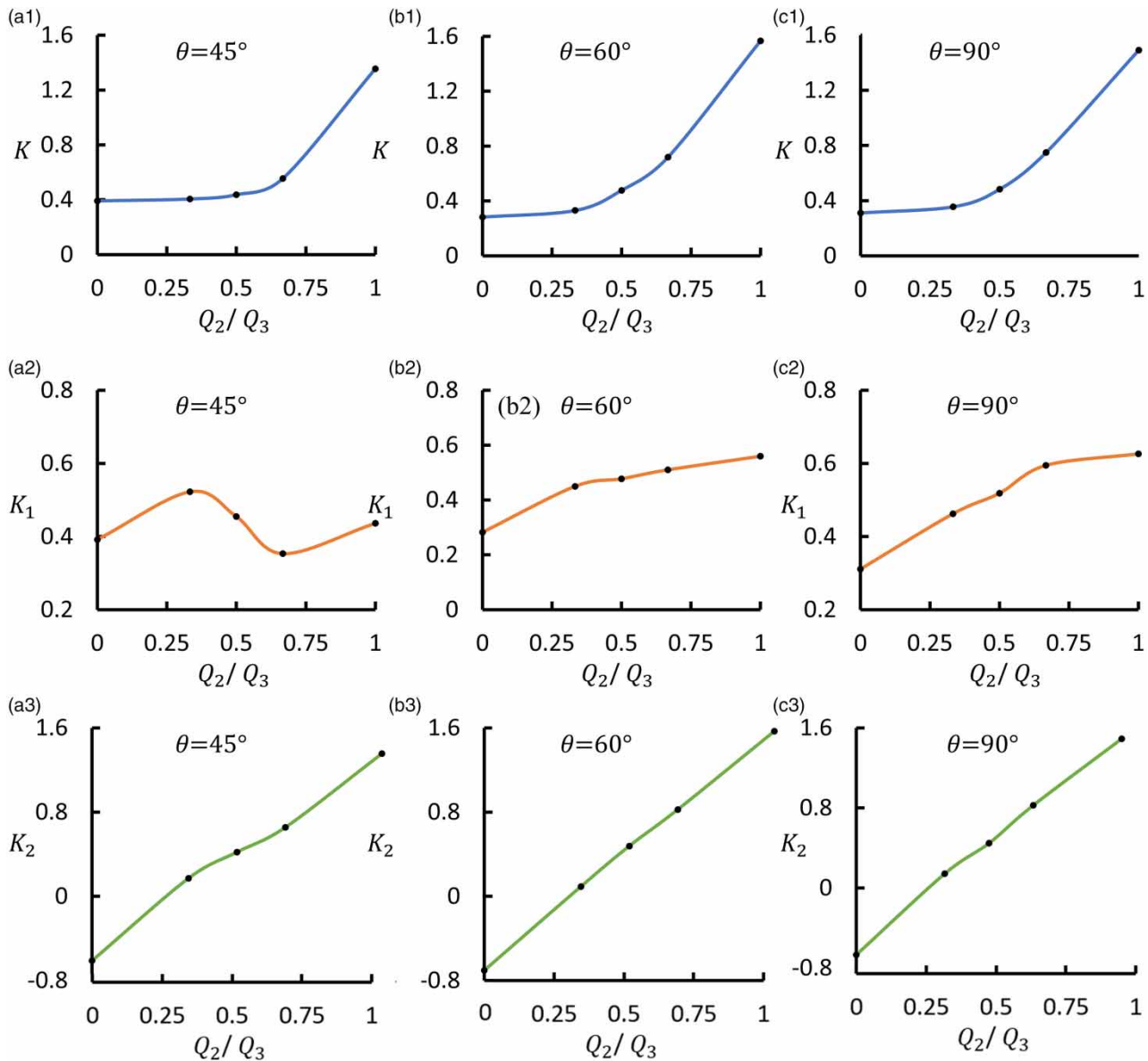


Figure 4 | The head loss coefficients K , K_1 , and K_2 with flow discharge ratio Q_2/Q_3 . (a1), (a2), and (a3) represent the head loss coefficient K , K_1 , and K_2 according to $\theta = 45^\circ$. (b1), (b2), and (b3) represent the head loss coefficient K , K_1 , and K_2 according to $\theta = 60^\circ$. (c1), (c2), and (c3) represent the head loss coefficients K , K_1 , and K_2 according to $\theta = 90^\circ$. The downstream water depth $h_d = 0.05\text{m}$.

manhole significantly increases with the increase of Q_2/Q_3 . When Q_2/Q_3 increases, the flow velocity distribution and vortex structure are both enhanced thus leading to an increased energy loss at the manhole.

4.3. Effect of connected angle on manhole energy loss

In this section, the influence of the connected angle θ between inflow pipes on total energy loss coefficient K at the manhole is discussed. Figure 8(a) shows the trend of the local energy loss with flow discharge ratio Q_2/Q_3 under different connected angles ($\theta = 45^\circ, 60^\circ, 90^\circ$). It is observed that the local energy loss coefficient K increases with the increase of Q_2/Q_3 . Moreover, there is a critical flow discharge ratio $Q_2/Q_3 = 0.5$ for the effect of connected angle θ on manhole local energy loss. When $Q_2/Q_3 < 0.5$, the total head loss coefficient K of the connected angle $\theta = 45^\circ$ is larger than that of $\theta = 60^\circ$ and $\theta = 90^\circ$. Conversely, when $Q_2/Q_3 > 0.5$, K of $\theta = 45^\circ$ is smaller than that of $\theta = 60^\circ$ and $\theta = 90^\circ$. Figure 8(b) shows the trend of the hydrodynamic force F along the main flow direction with flow discharge ratio Q_2/Q_3 under different connected

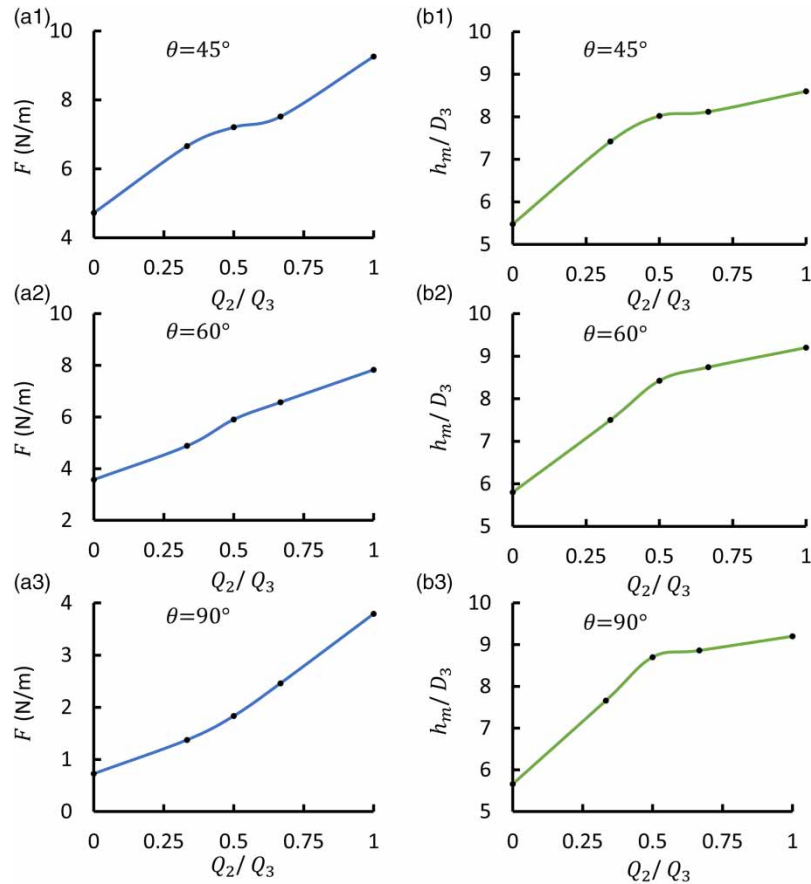


Figure 5 | Hydrodynamic force with flow discharge ratio Q_2/Q_3 in different conditions: (a1) $\theta = 45^\circ$, (a2) $\theta = 60^\circ$, and (a3) $\theta = 90^\circ$. Manhole water depth h_m with flow discharge ratio Q_2/Q_3 in different conditions: (b1) $\theta = 45^\circ$, (b2) $\theta = 60^\circ$, and (b3) $\theta = 90^\circ$. The downstream water depth $h_d = 0.05\text{m}$.

angles ($\theta = 45^\circ, 60^\circ, 90^\circ$). It is found that the F decreases when θ is increased from 45° to 90° . This trend is not fully consistent with the trend of the total head loss coefficient. To further analyze the phenomenon, Figure 9 shows the flow structure in the manhole by comparing the velocity distribution and streamline in horizontal cross-section with two different connected angles $\theta = 45^\circ$ and $\theta = 90^\circ$, respectively.

When the flow discharge ratio $Q_2/Q_3 = 1:3$, vortex flow structure area (streamline in the ellipse dotted line) at the manhole of $\theta = 45^\circ$ is larger than that of $\theta = 90^\circ$. Therefore, in this case, the local energy loss of $\theta = 45^\circ$ is bigger than that of $\theta = 90^\circ$. However, when the flow discharge ratio Q_2/Q_3 increasing from 1:3 to 2:3, the local energy loss of $\theta = 90^\circ$ is bigger than that of $\theta = 45^\circ$. This is because vortex flow structure at the manhole of $\theta = 90^\circ$ is enhanced and becomes stronger than that of $\theta = 45^\circ$, which dominates the local energy loss even though the hydrodynamic force term of $\theta = 45^\circ$ is larger than that of $\theta = 90^\circ$. Overall, the effect of connected angle θ on manhole local energy loss is influenced by the flow discharge ratio Q_2/Q_3 . When Q_2/Q_3 is smaller than 0.5, the local energy loss of the connected angle $\theta = 45^\circ$ is larger than that of $\theta = 60^\circ$ and $\theta = 90^\circ$. Conversely, if Q_2/Q_3 is larger than 0.5, the local energy loss of $\theta = 45^\circ$ is smaller than that of $\theta = 60^\circ$ and $\theta = 90^\circ$. It is noted that the enhanced vortex structure increases the local energy loss at the junction manhole.

4.4. Effect of manhole shape on manhole energy loss

In this section, the influence of the manhole cross-section shapes (square and circle) on total energy loss at the three-way junction manhole is discussed. Figure 10 displays the trend of the local energy loss coefficient K with flow discharge ratio Q_2/Q_3 at circular and square cross-section manholes, respectively. It is found that the local energy loss at the circular manhole is smaller than that of the square manhole. This is due to the boundary condition of the square manhole being sharper

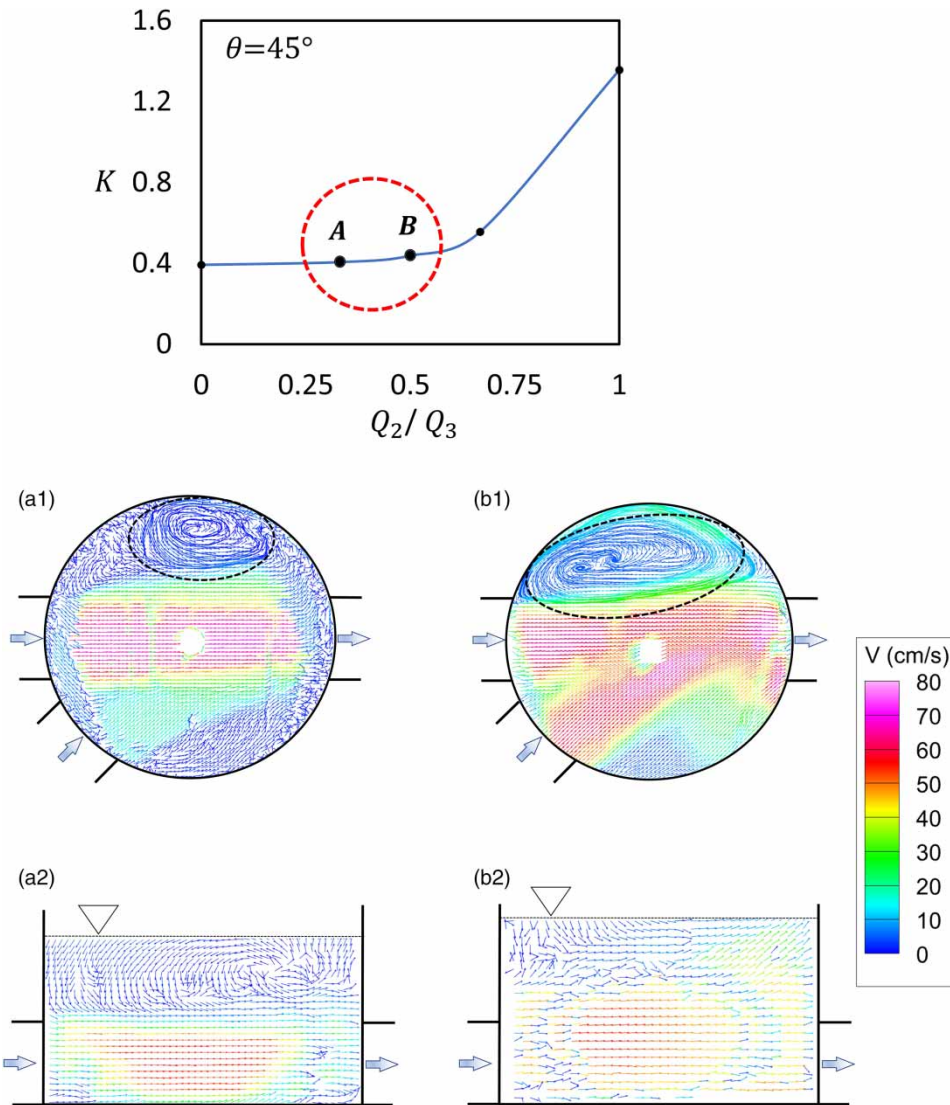


Figure 6 | Velocity distribution and streamline of two different flow discharge ratios Q_2/Q_3 when $\theta = 45^\circ$, (a1) horizontal cross-section at $y = 0.025$ m for $Q_2/Q_3 = 1:3$, (b1) horizontal cross-section at $y = 0.025$ m for $Q_2/Q_3 = 1:2$, (a2) vertical cross-section for $Q_2/Q_3 = 1:3$, (b2) vertical cross-section for $Q_2/Q_3 = 1:2$.

than that of the circular manhole, which will enhance the generation of turbulence and lead to the increase of the local energy loss. Manhole cross-section shape has an effect on the local energy loss; energy loss at the circular manhole is smaller than that of the square manhole.

4.5. Validation of empirical head loss coefficient formulae

The expression of the head loss coefficients provides an important tool for the design of urban drainage system and flood modelling. To validate the existing empirical head loss coefficient formulae, the head loss coefficients of a surcharged three-way junction manhole obtained from experiments were used to examine two empirical formulae by [FHWA \(2009\)](#) and [Arao et al. \(2016\)](#). Results in [Figure 11](#) show that the tendencies of the total head loss coefficients were in a relatively good agreement for both empirical formulae. It was observed that the formula proposed by [ARA0 et al. \(2016\)](#) performs better than the formula of UDDM for K and K_2 . However, the formula of UDDM has better accuracy than [ARA0 et al. \(2016\)](#) in terms of calculating K_1 .

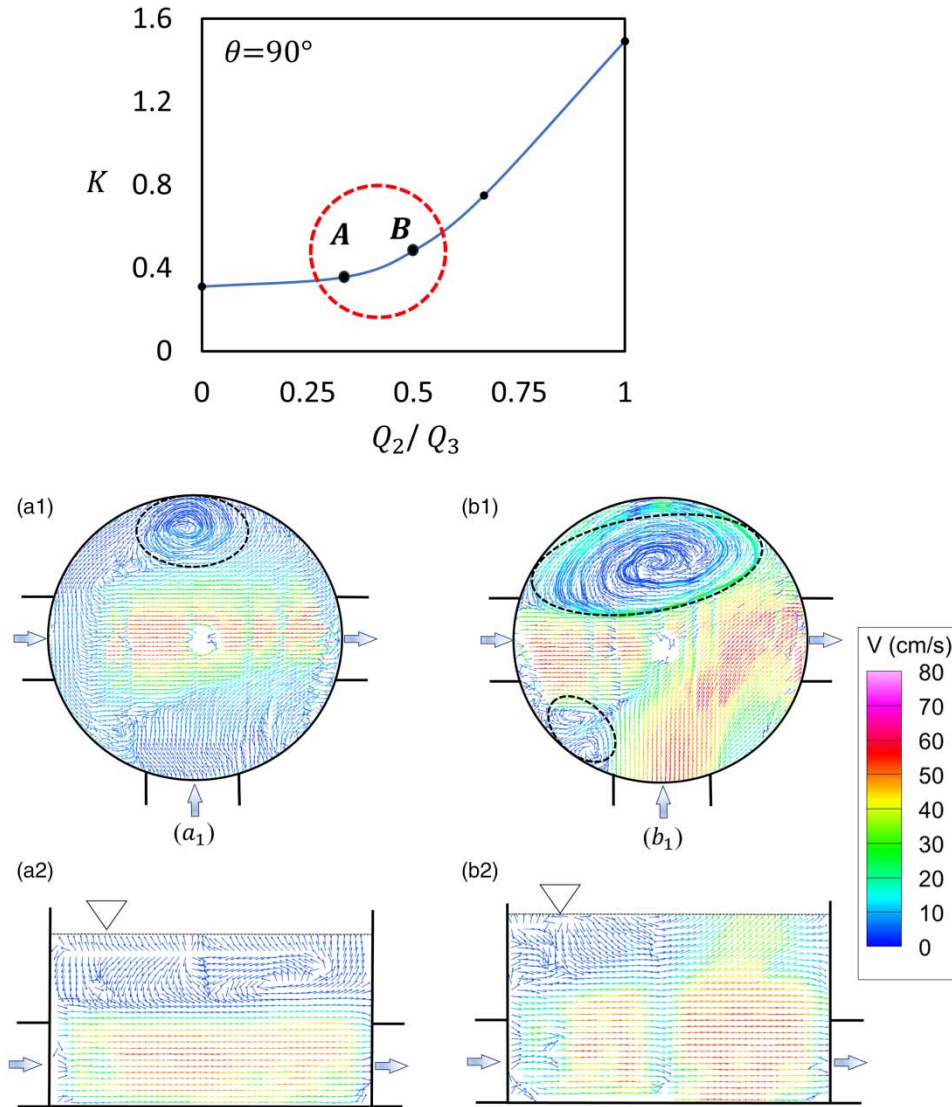


Figure 7 | Velocity distribution and streamline of two different flow discharge ratios when $\theta = 90^\circ$, (a1) horizontal cross-section at $y = 0.025$ m for $Q_2/Q_3 = 1:3$, (b1) horizontal cross-section at $y = 0.025$ m for $Q_2/Q_3 = 1:2$, (a2) vertical cross-section for $Q_2/Q_3 = 1:3$, (b2) vertical cross-section for $Q_2/Q_3 = 1:2$.

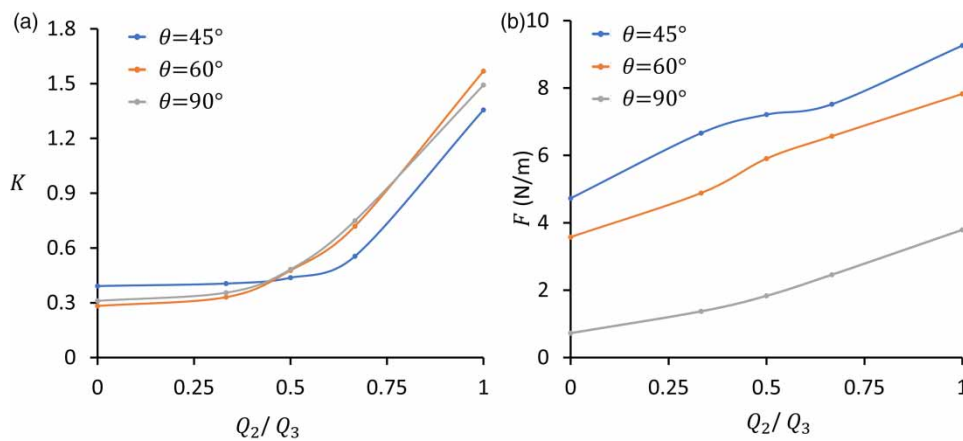


Figure 8 | Total energy loss coefficient (a) and resultant force F (b) with flow discharge ratio under three connected angles ($\theta = 45^\circ, 60^\circ, 90^\circ$).

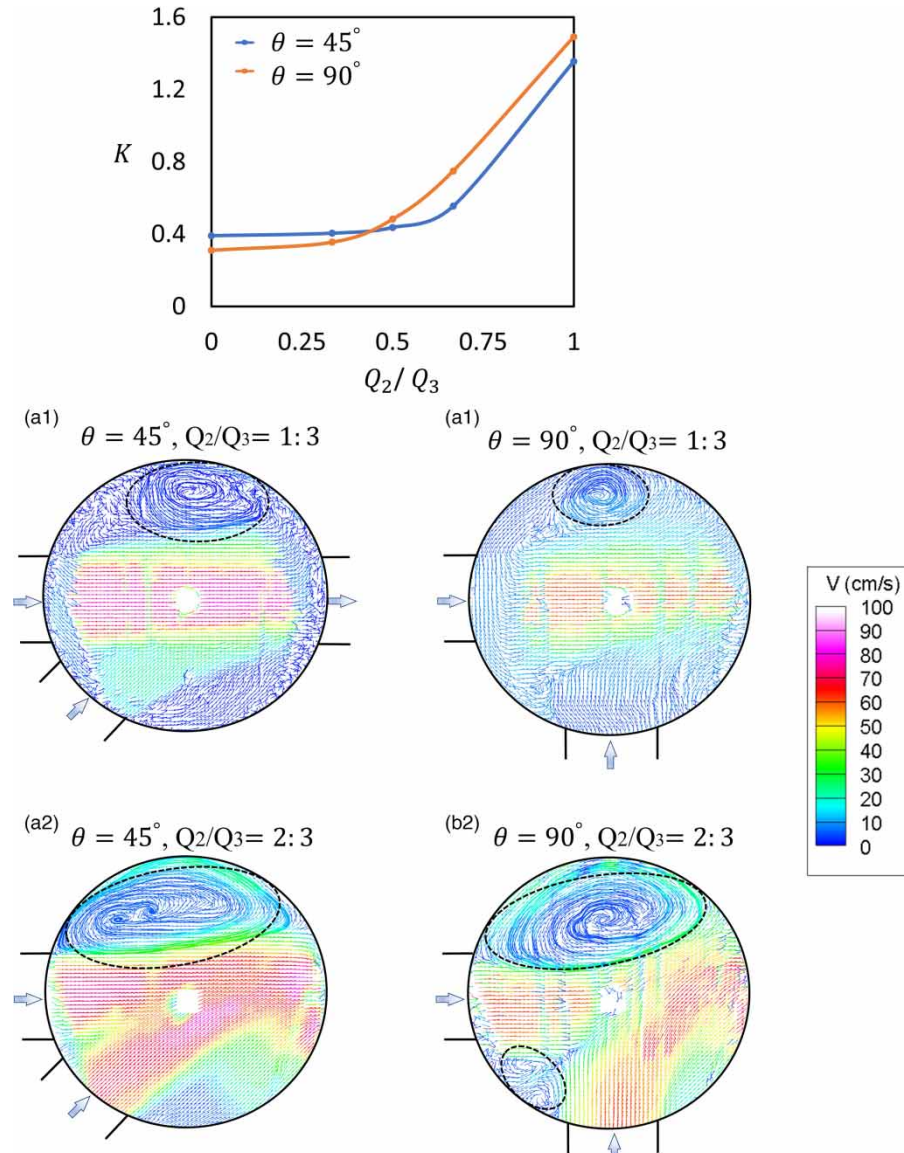


Figure 9 | Comparison of velocity distribution and streamline in horizontal cross-section at $y = 2.5$ cm with two different connected angles $\theta = 45^\circ$ and $\theta = 90^\circ$, respectively. (a1) $\theta = 45^\circ, Q_2/Q_3 = 1:3$, (b1) $\theta = 90^\circ, Q_2/Q_3 = 1:3$, (a2) $\theta = 45^\circ, Q_2/Q_3 = 2:3$, (b2) $\theta = 90^\circ, Q_2/Q_3 = 2:3$.

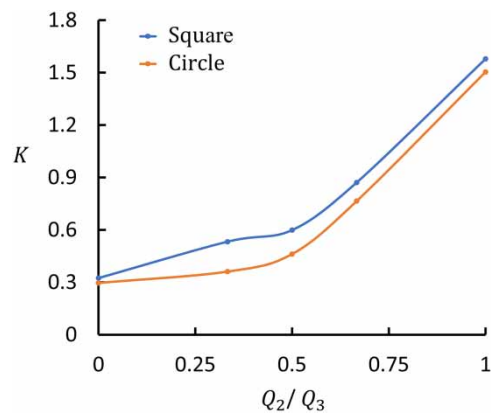


Figure 10 | Comparison of total energy loss coefficients with two different horizontal cross-section shape square and circle, respectively.

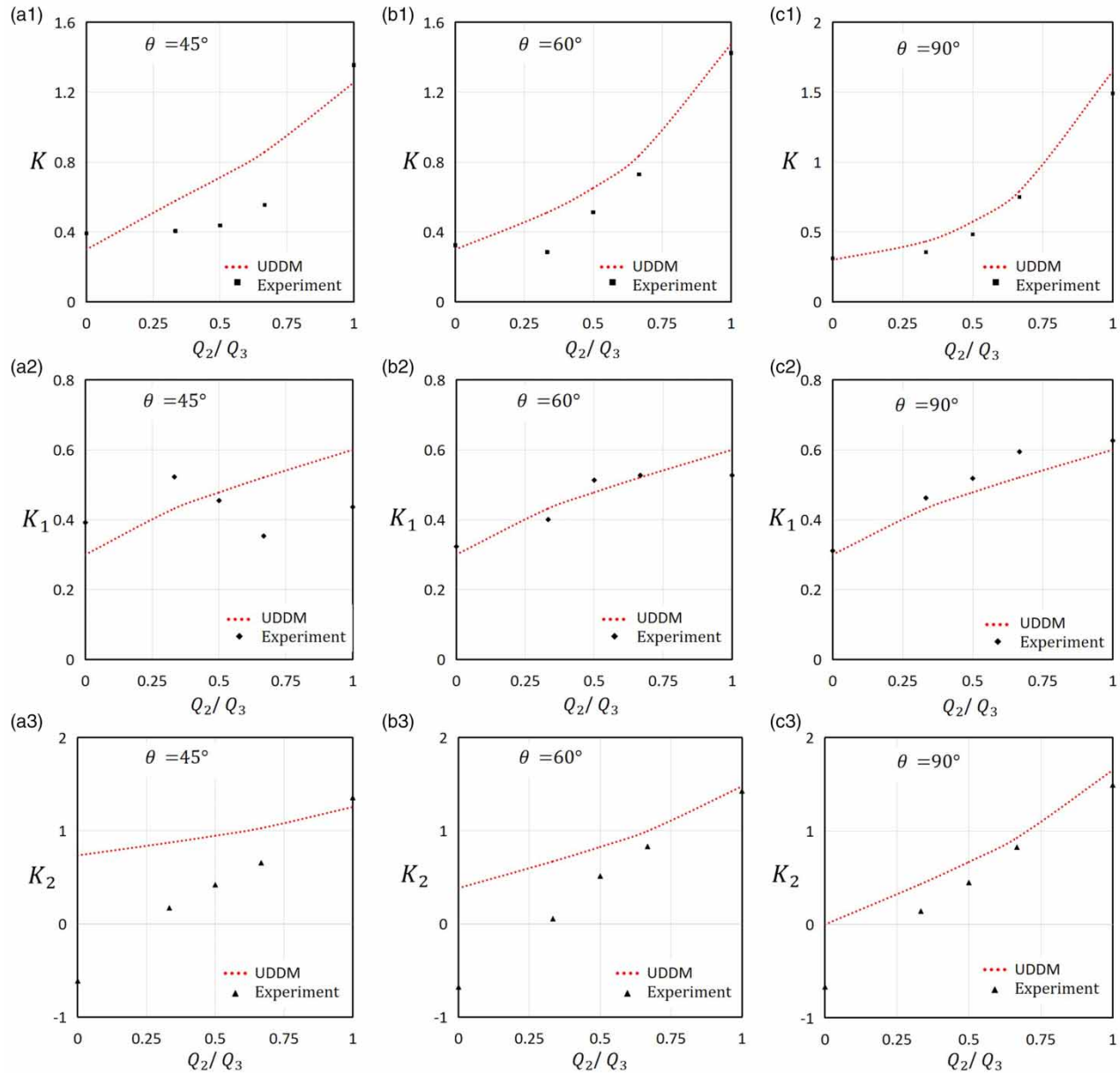


Figure 11 | Comparison of energy loss coefficients among two theoretical formulae (UDDM and ARAO *et al.* (2016)) and experimental results. When $\theta = 45^\circ$, (a1) shows the results of K , (a2) represents the results of K_1 , and (a3) shows the results of K_2 . Analogously, when $\theta = 60^\circ$, (b1), (b2), and (b3) show the results of K , K_1 , and K_2 , respectively. When $\theta = 90^\circ$, (c1), (c2), and (c3) show the results of K , K_1 , and K_2 , respectively.

To further examine the applicability of these two empirical formulae, the correlation between experimental and theoretical values were analyzed. Pearson correlation coefficients (R and R^2) were calculated to represent the correlation magnitudes. Figure 12 shows the scatter plot of correlation analysis between the experimental and theoretical results according to head loss coefficients K , K_1 , and K_2 , respectively. It is observed that both empirical formulae showed positive correlations. Correlation coefficients for K by UDDM and ARAO *et al.* are $R = 0.9578$ and $R = 0.9739$, respectively. Correlation coefficients for K_2 by UDDM and ARAO *et al.* are $R = 0.8876$ and $R = 0.9848$, respectively. This indicates that the accuracy of ARAO *et al.* is higher than that of UDDM in terms of calculating K and K_1 . However, it is also found that both formulae cannot fit well with the calculation of K_2 . Correlation coefficients for K_2 by UDDM and ARAO *et al.* are $R = 0.6796$ and $R = 0.4027$, respectively. The accuracy of UDDM is higher than that of ARAO *et al.* in terms of calculating K_2 .

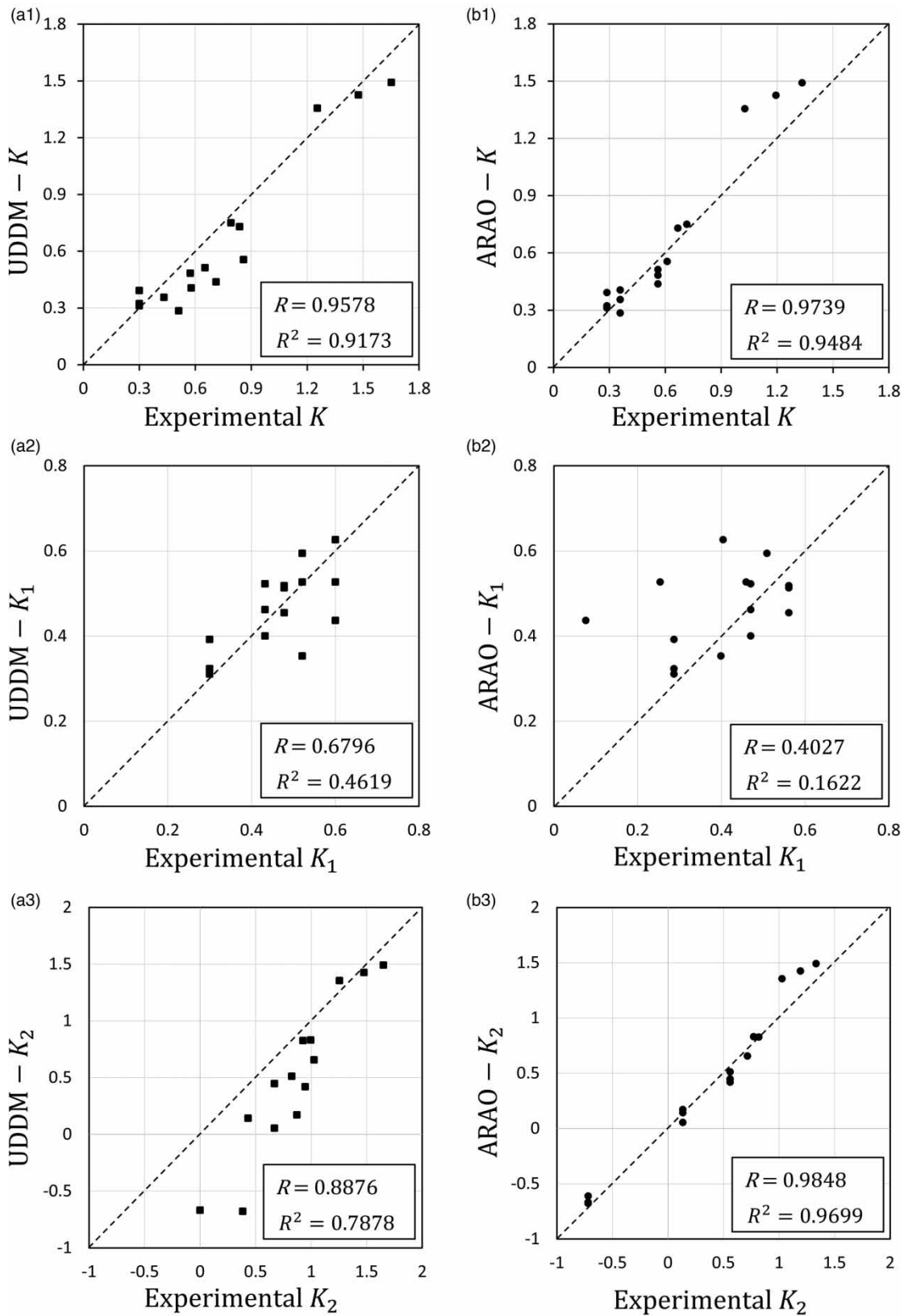


Figure 12 | Results of correlation analysis between the experimental results by the physical model and the empirical results by UDDM and ARAO et al. (2016) formulae. (a1), (a2), and (a3) show the comparison of K , K_1 , and K_2 between the experimental results and the calculated results by UDDM formulae. Analogously, (b1), (b2), and (b3) show the comparison of K , K_1 , and K_2 between the experimental results and the calculated results by ARAO et al. (2016) formulae.

5. CONCLUSIONS AND FUTURE WORKS

This paper presents an experimental study on local energy loss and flow structures at the surcharged three-way junction manhole according to the changes in the downstream water depth, the inlet flow rate ratio, the connected angle between two inlet pipes, and the manhole shape. Head loss coefficients K , K_1 , and K_2 at the surcharged three-way manholes were quantified and used to validate two empirical formulae.

The present work demonstrates that total head loss coefficient at the three-way junction manhole increases as the flow rate ratio was increased. There exists a critical flow discharge ratio $Q_2/Q_3 = 0.5$ for the effect of connected angle θ on the manhole local energy loss. Specifically, when $Q_2/Q_3 < 0.5$, the local energy loss value of the connected angle $\theta = 45^\circ$ is larger than that of $\theta = 60^\circ$ and $\theta = 90^\circ$. When $Q_2/Q_3 > 0.5$, the local energy loss value of the connected angle $\theta = 45^\circ$ is smaller than that of $\theta = 60^\circ$ and $\theta = 90^\circ$. In addition, it is also observed that the effect of downstream water depth on manhole local energy loss is insignificant for the studied cases.

Vortex structure was evident in the energy loss at the surcharged three-way manhole due to changes of hydraulic and geometrical parameters, including: (1) the increased flow discharge for junction manholes by the lateral inlet pipe; (2) the flow directional change of the inlet lateral pipe; and (3) the cross-sectional change of the manhole from circular to square. It is demonstrated that with the increase of the lateral inflow discharge, the flow velocity distribution and vortex structure are both enhanced and lead to obvious increased energy loss at the manhole. The enhanced vortex flow structure for different connected angles has a significant effect on the local energy loss with the increased flow discharge ratio. It is also found that a circular manhole can reduce local energy loss compared to the square manhole due to a less-sharp and smoother boundary, which reduces the effect of turbulent flow leading to a decrease in local energy loss.

Two empirical head loss coefficient equations were tested at the three-way surcharged manhole model. The equation of ARAO *et al.* (2016) performs better than the equation of UDDM in terms of calculating K and K_1 . However, the accuracy of UDDM is higher than ARAO *et al.* (2016) for calculating K_2 . Overall, these two empirical formulae fit well with the data measured on the physical model for the basic trend of the total head loss coefficients at the three-way surcharged manhole. The present results may potentially be useful to develop the design and validation of novel theoretical formulae for head loss coefficients.

Further investigations are expected to study other important aspects in the evaluation of the flow behavior of vortex flow structure and to develop efficient and accurate formulae for the calculation of energy loss coefficients. It is noted that the specific manhole configuration considered in this work is simpler than the practical manhole system, which may include benching. The study of energy loss in benched manhole system and future research to test the reliability of the empirical formulae will be desirable especially for practical engineering conditions.

ACKNOWLEDGEMENTS

This research work was supported by the National Natural Science Foundation of China (Grant Nos. 51725902, 41890820); the Royal Academy of Engineering through the Urban Flooding Research Policy Impact Programme (Grant No. UUFRIPI\100031); and the Newton Advanced Fellowships from the NSFC and the UK Royal Society (Grant Nos. 52061130219; NAF\R1\201156). This research was also supported by the JSPS KAKENHI Grants-in-Aid for Young Scientists (A) (Grant No. 16H06100) and the DPRI Collaborative Research Fund of Kyoto University (Grant No. 2019G-05). The authors thank the linguistic suggestions from Dr Syazana Omar. The authors would like to express their sincere thanks to the editor and anonymous referees for their valuable comments and suggestions.

DATA AVAILABILITY STATEMENT

All relevant data are included in the paper or its Supplementary Information.

REFERENCES

- Arao, S., Hiratsuka, S. & Kusuda, T. 2016 Formula on energy losses at three-way circular drop manhole under surcharge flow. *Journal of JSCE* 4 (1), 19–37. https://doi.org/10.2208/journalofjsce.4.1_19.
- Borsányi, P. *et al.* 2008 Modelling real-time control options on virtual sewer systems. *Journal of Environmental Engineering and Science* 7 (4), 395–410. <https://doi.org/10.1139/s08-004>.

- Chang, H. K. *et al.* 2013 Improvement of a drainage system for flood management with assessment of the potential effects of climate change. *Hydrolog Sci J* **58** (8), 1581–1597. doi:10.1080/02626667.2013.836276.
- Crispino, G., Cozzolino, L., Della Morte, R. & Gisonni, C. 2015 Supercritical low-crested bilateral weirs: hydraulics and design procedure. *Journal of Applied Water Engineering and Research* **3** (1), 35–42. doi:10.1080/23249676.2015.1026852.
- Crispino, G., Pfister, M. & Gisonni, C. 2019a Hydraulic design aspects for supercritical flow in vortex drop shafts. *Urban Water Journal* **16** (3), 225–234. doi:10.1080/1573062X.2019.1648531.
- Crispino, G., Pfister, M. & Gisonni, C. 2019b Supercritical flow in junction manholes under invert- and obvert-aligned set-ups. *Journal of Hydraulic Research* **57** (4), 534–546. doi:10.1080/00221686.2018.1494056.
- Crispino, G., Contestabile, P., Vicinanza, D. & Gisonni, C. 2021 Energy head dissipation and flow pressures in vortex drop shafts. *Water* **13** (2). doi:10.3390/w13020165.
- Del Giudice, G., Gisonni, C. & Hager Willi, H. 2000 Supercritical flow in bend manhole. *Journal of Irrigation and Drainage Engineering* **126** (1), 48–56. doi:10.1061/(ASCE)0733-9437(2000)126:1(48).
- FHWA 2009 *Urban Drainage Design Manual*. Hydraulic Engineering Circular, Washington DC, p. 22.
- Gisonni, C. & Hager, W. H. 2002 Supercritical flow in the 90° junction manhole. *Urban Water* **4** (4), 363–372. https://doi.org/10.1016/S1462-0758(02)00003-1.
- Granata, F., de Marinis, G. & Gargano, R. 2014 Flow-improving elements in circular drop manholes. *Journal of Hydraulic Research* **52** (3), 347–355.
- Jo, J. B., Kim, J. S. & Yoon, S. E. 2018 Experimental estimation of the head loss coefficient at surcharged four-way junction manholes. *Urban Water Journal* **15** (8), 780–789. doi:10.1080/1573062X.2018.1547408.
- Kim, J. S., Jo, J. B. & Yoon, S. E. J. W. 2018 Head loss reduction in surcharged four-way junction manholes. **10** (12), 1741.
- Lin, R., Zheng, F., Savic, D., Zhang, Q. & Fang, X. 2020 Improving the effectiveness of multiobjective optimization design of urban drainage systems. *Water Resources Research* **56** (7), e2019WR026656. https://doi.org/10.1029/2019WR026656.
- Lindvall, G. 1984 Head losses at surcharged manholes with a main pipe and a 90 lateral. In: *Proc. 3rd Int. Conf. on Urban Storm Drainage*, Goetborg, Sweden. Chalmers Univ. of Technology.
- Marsalek, J. 1984 Head losses at sewer junction manholes. *Journal of Hydraulic Engineering* **110** (8), 1150–1154. https://doi.org/10.1061/(ASCE)0733-9429(1984)110:8(1150).
- Pfister, M. & Gisonni, C. 2014 Head losses in junction manholes for free surface flows in circular conduits. *Journal of Hydraulic Engineering* **140** (9), 06014015. doi:10.1061/(ASCE)HY.1943-7900.0000895.
- Rubinato, M. *et al.* 2017 Experimental calibration and validation of sewer/surface flow exchange equations in steady and unsteady flow conditions. *Journal of Hydrology* **552**, 421–432. https://doi.org/10.1016/j.jhydrol.2017.06.024.
- Rubinato, M., Lee, S., Martins, R. & Shucksmith, J. D. 2018a Surface to sewer flow exchange through circular inlets during urban flood conditions. *Journal of Hydroinformatics* **20** (3), 564–576. doi:10.2166/hydro.2018.127.
- Rubinato, M., Martins, R. & Shucksmith, J. D. 2018b Quantification of energy losses at a surcharging manhole. *Urban Water Journal* **15** (3), 234–241. doi:10.1080/1573062X.2018.1424217.
- Ruggaber, T. P., Talley, J. W. & Montestruque, L. A. 2007 Using embedded sensor networks to monitor, control, and reduce CSO events: a pilot study. *Environmental Engineering Science* **24** (2), 172–182. https://doi.org/10.1089/ees.2006.0041.
- Stovin, V., Bennett, P. & Guymer, I. 2013 Absence of a hydraulic threshold in small-diameter surcharged manholes. *Journal of Hydraulic Engineering* **139** (9), 984–994. doi:10.1061/(ASCE)HY.1943-7900.0000758.
- Tavakol, D. H. *et al.* 2016 How does climate change affect combined sewer overflow in a system benefiting from rainwater harvesting systems? *Sustainable Cities and Society* **27**, 430–438. https://doi.org/10.1016/j.scs.2016.07.003.
- Wang, K. H., Cleveland, T. G., Towsley, C. & Umrigar, D. 1998 Head loss at manholes in surcharged sewer systems. *JAWRA Journal of the American Water Resources Association* **34** (6), 1391–1400. https://doi.org/10.1111/j.1752-1688.1998.tb05439.x.
- Zhang, M. *et al.* 2018 Quantifying rainfall-derived inflow and infiltration in sanitary sewer systems based on conductivity monitoring. *Journal of Hydrology* **558**, 174–183. https://doi.org/10.1016/j.jhydrol.2018.01.002.
- Zhang, H., Kawaike, K., Okada, S. & Fujiwara, T. 2020 Experimental study on hydraulic properties of manholes in a surcharged sewer pipe system. *Journal of Japan Society of Civil Engineers Ser A2* **76** (2), 451–460.
- Zheng, F., Li, Y., Zhao, J. & An, J. 2017 Energy dissipation in circular drop manholes under different outflow conditions. *Water* **9** (10). https://doi.org/10.3390/w9100752
- Zhu, Z., Chen, Z., Chen, X. & He, P. 2016 Approach for evaluating inundation risks in urban drainage systems. *Science of The Total Environment* **553**, 1–12. https://doi.org/10.1016/j.scitotenv.2016.02.025.

First received 27 September 2021; accepted in revised form 15 December 2021. Available online 29 December 2021